Solar Phys (2018) 293:30
https://doi.org/10.1007/s11207-018-1249-x

Relating Solar Energetic Particle Event Fluences to Peak Intensities

Stephen W. Kahler[1] · **Alan G. Ling**[2]

Received: 17 October 2017 / Accepted: 12 January 2018

Abstract Recently we (Kahler and Ling, *Solar Phys.* **292**, 59, 2017: KL) have shown that time–intensity profiles [$I(t)$] of 14 large solar energetic particle (SEP) events can be fitted with a simple two-parameter fit, the modified Weibull function, which is characterized by shape and scaling parameters [α and β]. We now look for a simple correlation between an event peak energy intensity [$I_{\rm p}$] and the time integral of $I(t)$ over the event duration: the fluence [F]. We first ask how the ratio of $F/I_{\rm p}$ varies for the fits of the 14 KL events and then examine that ratio for three separate published statistical studies of SEP events in which both F and $I_{\rm p}$ were measured for comparisons of those parameters with various solar-flare and coronal mass ejection (CME) parameters. The three studies included SEP energies from a 4 – 13 MeV band to $E > 100$ MeV. Within each group of SEP events, we find a very robust correlation (CC > 0.90) in log–log plots of F *versus* $I_{\rm p}$ over four decades of $I_{\rm p}$. The ratio increases from western to eastern longitudes. From the value of $I_{\rm p}$ for a given event, F can be estimated to within a standard deviation of a factor of ≤ 2. Log–log plots of two studies are consistent with slopes of unity, but the third study shows plot slopes of < 1 and decreasing with increasing energy for their four energy ranges from $E > 10$ MeV to > 100 MeV. This difference is not explained.

Keywords Energetic particles · Acceleration

1. Introduction

Solar energetic ($E \gtrsim 10$ MeV) particle events observed in space are characterized principally by their peak intensities at standard differential or integral energies. Perhaps the

✉ S.W. Kahler
stephen.kahler@us.af.mil

A.G. Ling
aling@aer.com

1 Space Vehicles Directorate, Air Force Research Laboratory, 3550 Aberdeen Ave., Kirtland AFB, NM 87117, USA

2 Atmospheric Environmental Research, 2201 Buenta Vista Drive SE, Suite 407, Albuquerque, NM 87106, USA

Published online: 01 February 2018

most common standard is the NOAA Space Weather Prediction Center list of Solar Proton Events Affecting the Earth Environment umbra.nascom.nasa.gov/SEP/ for all solar energetic particle (SEP) events reaching intensities of 10 pfu [proton flux units: 1 p(cm^2 s sr)$^{-1}$] as measured on the NOAA *Geostationary Operational Environmental Satellites* (GOES) spacecraft. SEP-event peak intensities [I_p] are widely used in studies to determine their solar origins in flares or coronal mass ejections (CMEs: Cane, Richardson, and von Rosenvinge, 2010; Kahler, 2013; Miteva *et al.*, 2013; Gopalswamy *et al.*, 2014, 2015; Park and Moon, 2014; Richardson *et al.*, 2014; Takahashi, Mizuno, and Shibata, 2016). Work on spatial distributions of SEP event I_p (Lario *et al.*, 2013) and their dependence on solar-wind characteristics (Lario and Karelitz, 2014; Kahler and Vourlidas, 2014) has been based on their observed I_p. Validations of SEP forecast models (Posner, 2007; Balch, 2008; Laurenza *et al.*, 2009; Belov, 2009; Falconer *et al.*, 2011; Kahler, Ling, and White, 2015; Kahler, White, and Ling, 2017) often take events with I_p above a given threshold, typically 10 pfu at > 10 MeV, as the forecast targets.

For several kinds of studies, however, the SEP I_p-values are not adequate, and the time–intensity profiles [$I(t)$], which result from the convolution of SEP acceleration and transport processes, are needed. Determinations of average elemental abundances in SEP events (Schmelz *et al.*, 2012; Reames, 2014) and their spatial distributions (Cohen, Mason, and Mewaldt, 2017) require event fluences [F], the integration of intensity [$I(t)$] over the event durations, because the abundance ratios typically vary throughout the individual events (Mason *et al.*, 2012; Zelina *et al.*, 2017), and for heavy elements, the counting rates are usually low, particularly in the impulsive SEP events (Reames, Cliver, and Kahler, 2014; Reames, 2015). Integrations over entire SEP events in both time and energy are needed for comparisons of the SEP event energies with the overall energy budgets of solar eruptive events involving CMEs (Chollet, Giacalone, and Mewaldt, 2010; Emslie *et al.*, 2012; Aschwanden *et al.*, 2017) and separately with associated CME energies (Mewaldt *et al.*, 2008; Kahler and Vourlidas, 2013; Aschwanden *et al.*, 2017) to test the diffusive shock-acceleration mechanism.

Efforts to forecast SEP events are also evolving from the models, listed above, to forecast simple event occurrences or I_p to models designed to produce SEP profiles [$I(t)$]. The latter may use only profiles and disk locations of solar X-ray flares with (Ji, Moon, and Park, 2014; Papaioannou *et al.*, 2016) or without (Marsh *et al.*, 2015) associated CMEs as inputs. More sophisticated efforts take solar-wind flows and shocks driven by fast CMEs as model inputs (Verkhoglyadova *et al.*, 2010; Schwadron *et al.*, 2014; Pomoell *et al.*, 2015; Luhmann *et al.*, 2010, 2017; Bain *et al.*, 2016).

The dependence of SEP event F on I_p as functions of solar source longitudes and of SEP energies would be useful for both space-weather forecasting and for insights into the coupled physics of SEP acceleration and transport. Given the complexity of the acceleration process at shocks, driven by CMEs with a range of speeds and widths, and variations in particle scattering and transport, we might expect poor correlations between F and I_p over many SEP events. A simple first-order approximation for the fluence of an event is to take the product of I_p and an effective event duration timescale. For his comparison of 20-MeV SEP events and associated CMEs, Kahler (2013) defined TD as the duration of a SEP event when $I > 0.5I_p$. He compared event TD timescales in five separate source-longitude ranges and found the highest median value, 26 hours, in the E130° – E06° range and lowest value, 12 hours, in the two bins covering W33° – W90°. However, a confounding additional result was that TD was positively correlated with I_p for well-connected (W33° – W60°) events and negatively correlated with poorly connected (E130° – E06° and W100° – west limb) events, which calls into question the validity of the simple $I_p \times$ TD approximation for the event F.

We are not aware of any alternative statistical studies to compare F and I_p for SEP events, either as functions of SEP energy or of solar-source longitude. In the following sections we examine several published works to address this question.

2. The Modified Weibull Function and SEP Event Fluence

Kahler and Ling (2017, hereafter KL) have explored techniques for characterizing SEP event $I(t)$-profiles with two-parameter fits, and now we extend that work to a comparison of fluences F with I_p for a range of SEP events. KL sought simple two-parameter fits to the intensity profiles of 14 large SEP events. They considered several candidate probability distribution functions (PDFs) for which they replaced the parameter variable $[x]$ with the intensity profile time $[t]$. They chose the modified Weibull function

$$W'(t) = (-\alpha/\beta)(t/\beta)^{\alpha-1}\exp\left[-(t/\beta)^{\alpha}\right], \tag{1}$$

where t is the time from event onset, $\alpha < 0$ is the parameter that defines the profile shape, and β is the scaling parameter that stretches or compresses the basic shape of the event along the t-axis. The rise portions of the curves become extremely steep as $\alpha \Rightarrow 0$. The applicable range of α is ≈ -0.40 to -3.00. Whether $W'(t)$ should be equated to $\log I(t)$-values or to $I(t)$-values was decided in favor of $\log I(t)$ because of the large dynamic ranges of most SEP events. Using $W'(t) = I(t)$ produces good least-squares fits at high values of $I(t)$ but poor, even terrible, fits when $I(t)$ is several orders of magnitude smaller. An alternative function, the lognormal distribution, was not ruled out as a viable candidate when KL carried out their comparisons of lognormal and modified Weibull functions $W'(t)$ as fits for the $E > 10$, > 50, and > 100 MeV $\log I(t)$-profiles of three large SEP events.

KL showed examples of SEP events for which the qualities of fits were dependent on the time intervals of the profiles used in the fits. Their fits of α and β to the 14 SEP events generally satisfied the intuitive expectation that the scaling parameter $[\beta]$, reflecting the event durations, was larger for lower energies and for more poorly connected events. The α-parameter, on the other hand, showed only weak dependence on either energy or solar-source longitude.

An advantage of the Weibull PDF is that it is analytically integrable to calculate cumulative distribution functions (CDFs), see also Wilks (2006). $W'(t)$ can also be integrated to infinite t to obtain the equivalent cumulative total value of $\int W'(t)\,dt = \int \log I(t)\,dt$. Here we invert the process to calculate $\log I_p$ as a function of α and β for an assumed total cumulative value of $\int \log I(t)\,dt = 1$ and show the result in Figure 1. For a given β, $\log I_p$ is minimum at $\alpha = -0.806$. As expected, higher values of β result in smaller $\log I_p$ relative to the normalized CDF values. Moreover, lower values of α, with narrower profile peaks, have higher $\log I_p$. For the total of 42 SEP profile fits of KL, $-1.8 \le \alpha \le -0.3$ and $0.4 \le \log\beta \le 1.8$, which corresponds to a range of about one decade in Figure 1. We plot against the curves the 14 points corresponding to the α- and β-values derived for the $E > 50$ MeV profiles of KL.

We have to be careful to distinguish between SEP linear counting rates $[I(t)]$ and $\log I(t)$. The latter were the basis of the calculations of Figure 1 with $W'(t)$ and give relatively high weights to low counting rates compared to direct linear values $[I(t)]$. While the log curves of Figure 1 might imply huge variations in linear values of I_p compared to events of fixed fluences $[F]$, we can really test that implication only by comparing calculated SEP event values of F with their observed values I_p. In such comparisons we can look for systematic variations of F *versus* I_p as the SEP energies and source regions vary.

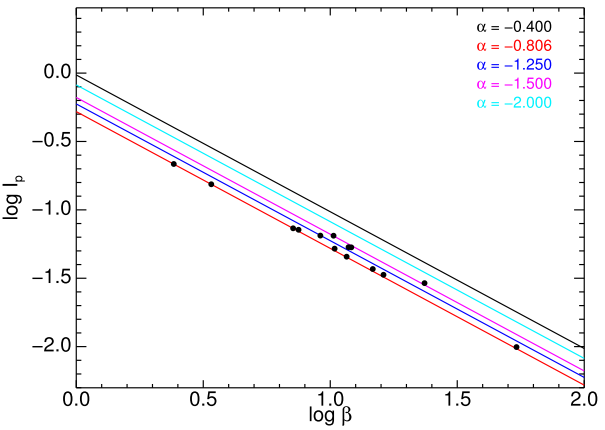

Figure 1 Values of log I_p *versus* log of the scaling parameter $[\beta]$ calculated for assumed fixed values of unity for the CDF of the modified Weibull function W' fit to $\int \log I(t)\,dt$. Plots are *color-coded* to show selected values of the shape parameter $[\alpha]$ in the range found for the SEP events of KL. The plot at $\alpha = -0.806$ is the minimum value for all α. *Data points* are the 14 $E > 50$ MeV SEP event fits from KL.

3. Data Analysis

SEP event F are often calculated for the purposes described in Section 1, and they are then compared with associated solar or SEP model driver inputs, but not with their own associated I_p-values. We here report three such comparisons, each from different authors with their own selected SEP energy ranges and event lists. The goal is to see how tightly the event F- and I_p-values are correlated and whether they have energy and/or solar source–longitude dependencies.

3.1. The *Helios* Era Lario *et al.* (2006) SEP Events

Lario *et al.* (2006) carried out a comprehensive comparison of 72 SEP differential I_p and event F with the *Helios* 1 and 2 and *Interplanetary Monitoring Platform* (IMP) 8 observations to determine SEP radial and longitudinal distributions. They used hourly averages of 4 – 13 and 27 – 37 MeV proton channels of *Helios* and generated comparable differential energy intensities from the *Charged Particle Measurement Experiment* on the IMP 8 spacecraft. They examined SEP events over the years 1976 – 1982, for which they obtained both I_p and F for the three spacecraft where possible. For our purposes we are interested only in their Table 2 IMP 8 observations, because we wish to perform comparisons only at 1 AU and not at the inner heliospheric locations of the *Helios* spacecraft.

Lario *et al.* (2006) selected the event prompt peaks or intensity plateaus and avoided using shock peaks. The values of F were calculated by subtracting the preexisting intensities in the two energy channels, and integrations were carried out until the intensities reached the pre-event level or a new particle injection occurred well into the decay phase. Values of F could not be determined for 18 of the 4 – 13 MeV events and for 22 of the 27 – 37 MeV proton events. Figure 2 shows plots of their calculated F *versus* I_p on log–log plots. The correlation coefficients (CCs) exceed 0.90 in both cases. The lower CC of 0.90 for the 27 – 37 MeV plot of Figure 2 is due to two high-F outliers on 16 February 1979 from an E59° source and on 8 September 1979 with an unattributed source location. The 27 – 37 MeV plot is consistent with a slope of unity, but the slope is significantly higher for the 4 – 13 MeV events. The main result, however, is that for a given SEP event from the Lario *et al.* (2006) study, F can be accurately estimated to within a factor of two from the observed I_p.

We have further divided the sources of the 54 4 – 13 MeV events and 50 27 – 37 MeV events into three solar longitude ranges of roughly equal numbers to look for any longitudinal effects in the $F - I_p$ association. Some SEP events were not associated with solar source

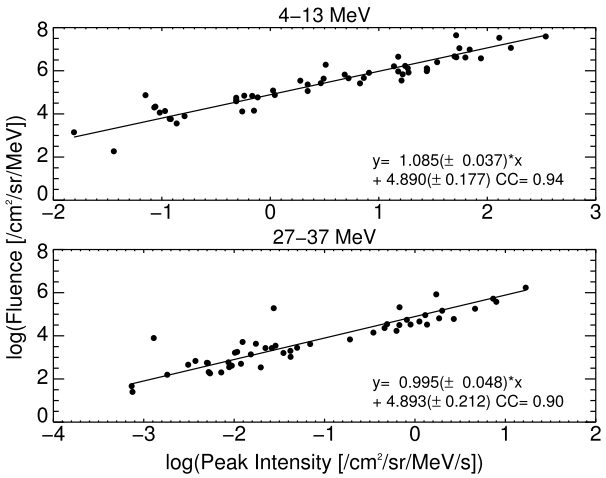

Figure 2 *Top*: Log–log plot of 4 – 13 MeV proton event differential F *versus* corresponding peak differential I_p for 54 IMP 8 events of Lario *et al.* (2006) with the least-squares linear best fit and CC. *Bottom*: Same for their 50 IMP 8 27 – 37 MeV proton events.

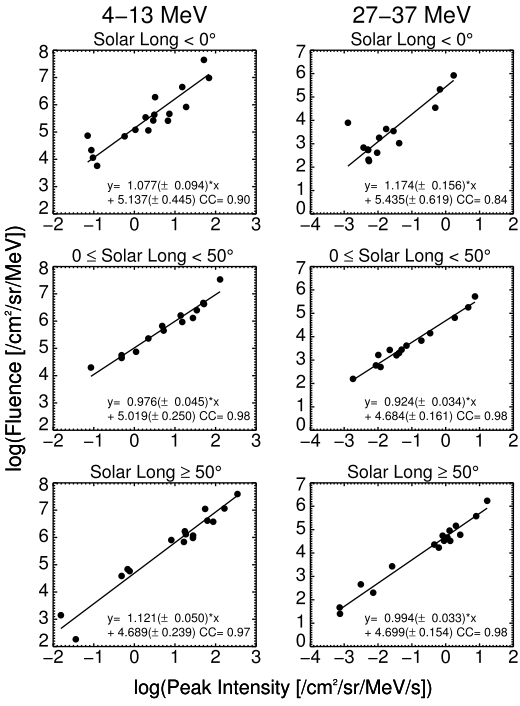

Figure 3 *Left side*: Log–log plots of the IMP-8 4 – 13 MeV proton differential F *versus* corresponding peak differential I_p for the 48 proton events of Lario *et al.* (2006) with known solar-source longitudes. From *top* to *bottom*, the panels show roughly similar numbers of events divided into three solar-source longitude ranges. *Right side*: Same for their 44 IMP-8 27 – 37 MeV proton events with known solar-source longitudes.

longitudes, leaving 48 4 – 13 MeV events and 44 27 – 37 MeV events with source attributions. In the plots shown in Figure 3 there are no obvious longitudinal trends in either the slopes or CCs for either energy range. We give in Table 1 the best-fit slopes and amplitudes and CCs for these and all other $F - I_p$ fits.

To look for amplitude variations with source longitude, but independent of the associated slope variations, we assumed slopes of unity for each event group and then did least-squares best fits to determine the resulting amplitudes best suited to determine the corresponding F

Table 1 Fit parameters to SEP event plots.

Source event years	Source long.	Energy range	Number events	Plot slope	Plot amplitude	Corr. coeff.	Unity slope amplitude
Lario *et al.*	All	4 – 13 MeV	54	1.09 ± 0.04	4.89 ± 0.18	0.94	4.93 ± 0.05
IMP 8		27 – 37 MeV	50	1.00 ± 0.05	4.89 ± 0.21	0.90	4.90 ± 0.07
1976 – 1982	EL – CM	4 – 13 MeV	17	1.08 ± 0.09	5.14 ± 0.45	0.90	5.16 ± 0.11
		27 – 37 MeV	14	1.17 ± 0.16	5.44 ± 0.62	0.84	5.15 ± 0.16
	CM – W50	4 – 13 MeV	14	0.98 ± 0.05	5.02 ± 0.25	0.98	5.00 ± 0.06
		27 – 37 MeV	14	0.92 ± 0.03	4.68 ± 0.16	0.98	4.77 ± 0.05
	W50 – WL	4 – 13 MeV	16	1.12 ± 0.05	4.69 ± 0.24	0.97	4.79 ± 0.09
		27 – 37 MeV	16	0.99 ± 0.03	4.70 ± 0.15	0.98	4.70 ± 0.06
Kahler *et al.*	All	> 50 MeV	125	1.08 ± 0.02	5.51 ± 0.14	0.94	5.61 ± 0.03
GOES	EL – W18	> 50 MeV	42	1.08 ± 0.05	5.56 ± 0.29	0.92	5.67 ± 0.07
1986 – 2016	W21 – W65	> 50 MeV	42	1.08 ± 0.03	5.47 ± 0.18	0.97	5.57 ± 0.04
	W67 – WL	> 50 MeV	41	1.08 ± 0.04	5.50 ± 0.21	0.96	5.60 ± 0.04
Papaioannou *et al.*	All	> 10 MeV	314	0.94 ± 0.01	4.85 ± 0.07	0.94	4.75 ± 0.02
GOES		> 30 MeV	228	0.88 ± 0.02	4.98 ± 0.09	0.94	4.86 ± 0.02
1984 – 2013		> 60 MeV	172	0.82 ± 0.02	5.01 ± 0.12	0.91	4.90 ± 0.03
		> 100 MeV	122	0.77 ± 0.02	4.93 ± 0.15	0.90	4.83 ± 0.03
	EL – CM	> 10 MeV	90	0.88 ± 0.02	5.01 ± 0.14	0.95	4.82 ± 0.03
		> 30 MeV	58	0.86 ± 0.03	5.11 ± 0.18	0.94	4.99 ± 0.04
		> 60 MeV	34	0.80 ± 0.03	5.18 ± 0.22	0.95	5.08 ± 0.06
		> 100 MeV	23	0.64 ± 0.05	5.14 ± 0.37	0.90	5.04 ± 0.09
	CM – W50	> 10 MeV	83	0.95 ± 0.02	4.73 ± 0.14	0.95	4.65 ± 0.03
		> 30 MeV	64	0.93 ± 0.03	4.87 ± 0.15	0.95	4.80 ± 0.03
		> 60 MeV	55	0.85 ± 0.03	4.96 ± 0.19	0.93	4.89 ± 0.04
		> 100 MeV	35	0.84 ± 0.04	4.84 ± 0.21	0.94	4.80 ± 0.05
	W50 – WL	> 10 MeV	89	1.01 ± 0.02	4.71 ± 0.11	0.97	4.72 ± 0.02
		> 30 MeV	72	0.91 ± 0.02	4.89 ± 0.13	0.96	4.77 ± 0.03
		> 60 MeV	59	0.83 ± 0.03	4.93 ± 0.18	0.94	4.77 ± 0.04
		> 100 MeV	51	0.77 ± 0.03	4.88 ± 0.21	0.92	4.75 ± 0.04

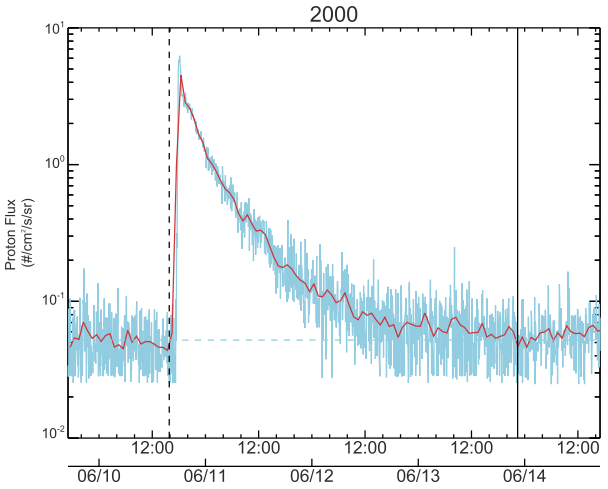

Figure 4 $E > 50$-MeV GOES proton profile showing the five-minute (*blue*) and hourly (*red*) $I(t)$ for a sample event. The fluence integration of this KWL event began at the onset (*vertical dashed line*) and ended at the time of the *vertical solid line*.

for any given SEP event I_p. These amplitudes and standard deviations are given in the last two columns of Table 1.

3.2. The $E > 50$ MeV SEP Events of the PPS Validation

In a recent work, Kahler, White, and Ling (2017, hereafter KWL) validated the proton prediction system (PPS) used by the US Air Force. This exercise used as the forecast goal 67 $E > 50$ MeV SEP events observed with the *Energetic Particle Sensor* (EPS) onboard the GOES spacecraft from 1986 to 2016 with $I_p \geq 10$ pfu. An additional 71 small (1 pfu $< I_p < 10$ pfu) 50-MeV events were also considered for those cases in which a small event was associated with a PPS false-alarm forecast of a 10 pfu SEP event. Here we reexamine the 71 small events and delete four cases that were not due to onsets of new events. Another five small events and four 10 pfu events could not be associated with solar-flare longitudes and were also deleted, leaving 125 of the 138 original events for the current analysis.

We have calculated the fluences of these 125 events, as did Lario *et al.* (2006) for their events, by subtracting from $I(t)$ the background counting rates at the times of SEP event onsets, ending only when $I(t)$ returned to background level or until another SEP event intervened. An example of an event on 10 June 2000 with superposed five-minute and hourly averages is shown in Figure 4. The dashed-green line shows the background calculated from the pre-event counting rate, which for the $E > 50$ MeV channel of the GOES proton detector is normally $\leq 10^{-1}$ pfu. The integration of $I(t)$ was terminated on 13 June at the time indicated by the vertical line. Since all of the SEP events of this study required $I_p > 1$ pfu, we find, as did Lario *et al.* (2006) in their study, that the background corrections make only minor reductions to the calculated values of F. For the event of Figure 4, the background correction to F is only 0.91% despite the extended low-intensity decay over the last half of the event. Corrections for all but two of the events' F were $< 4\%$, and the median correction for all events was only 0.40%.

The log–log $F - I_p$ plot for all 125 events of the PPS study is shown in Figure 5. The events are divided into three longitude ranges shown in Figure 6. The 14 large SEP events selected by KL for their intensity-profile fitting analysis are included in Figures 5 and 6, indicated with crosses. These events appear as typical of all the events in each longitude range. In particular, KL distinguished between the two extreme SEP events of 17 May 2012

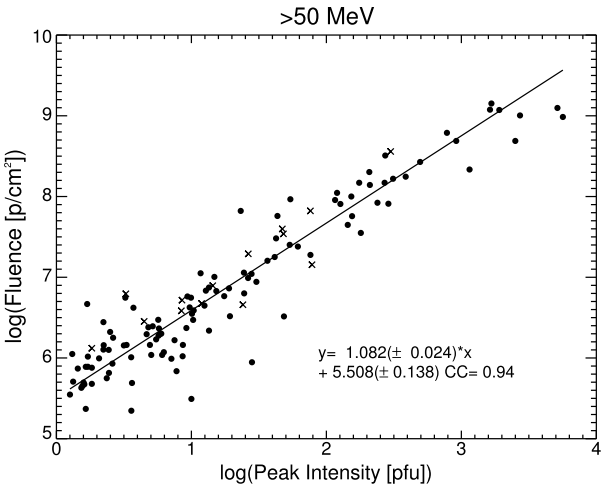

Figure 5 Background-corrected F *versus* I_p of the 125 $E > 50$ MeV proton events of KWL. The event minimum I_p is 1 pfu, and crosses are the 14 events from KL. The *solid line* is the least-squares best fit.

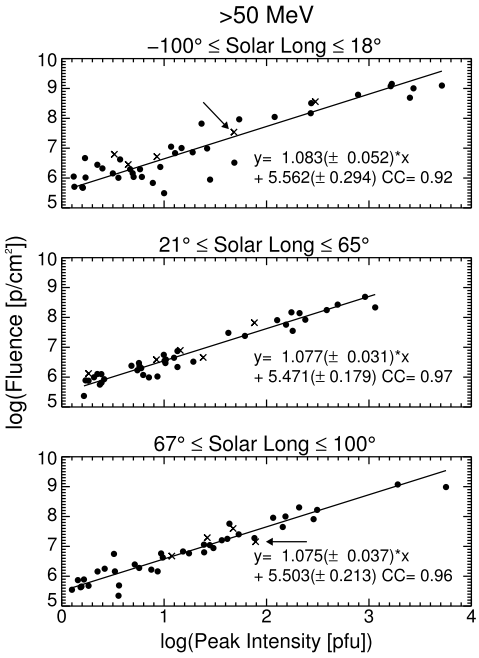

Figure 6 $F-I_p$ plot of Figure 5 divided into three longitude ranges of solar source regions. The least-squares fits of the separate plots are consistent with a common fit shown in Figure 5. This implies that there are no longitude effects on the relationship. *Crosses* are the KL events, and *arrows* in the *top* and *bottom panels* indicate the two events discussed in the text.

(W76°, $\log I_p = 1.89$), with an impulsive profile, and 7 January 2014 (W07°, $\log I_p = 1.69$), with a gradual profile. These two events, indicated by arrows in Figure 6, show that their fluences are only slightly below and above, respectively, the best-fit lines and do not constitute extreme displacements. We might expect a tendency for all SEP events to have a tight correlation in Figures 5 and 6 if there were a trend for more gradual SEP profiles (more negative α) to correlate with shorter event durations (smaller β). We have examined this possibility with plots of β *versus* α for the three energy ranges of the 14 event fits of KL. In all three cases there was no correlation between β and α.

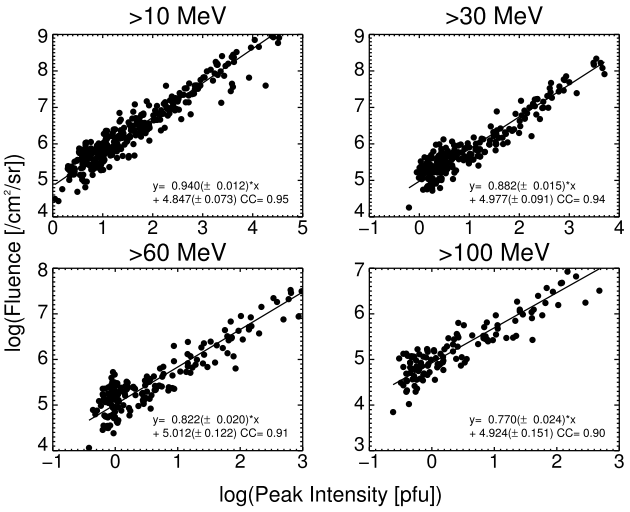

Figure 7 Log F *versus* log I_p for the four integral energy bands of the SEP events of the Papaioannou *et al.* (2016) catalog.

3.3. The Multiple-Energy SEP Events of Papaioannou *et al.* (2016)

Papaioannou *et al.* (2016) carried out an extensive statistical comparison of properties of SEP events with their associated flares and CMEs. To identify SEP events they began with a procedure to produce a continuous GOES data set of redefined differential energy channels obtained from cross-calibrations of the GOES *Space Environment Monitor* (SEM) and the IMP-8 GME data (Sandberg *et al.*, 2014). They developed a code to produce a rebinned data set in the range 7.23 – 10.46 MeV and searched for candidate events that exceeded a minimum peak of 0.5 pfu with a minimum waiting time between events and a duration of two hours to produce 291 candidate events. After another pass through the data with differential $I(t)$ from 4 to 500 MeV and a manual separation of candidates, they obtained a total of 314 SEP events in the 1996 to 2013 period. Rebinning their data into 100 logarithmically spaced channels within the energy range 5 – 500 MeV, they calculated for each event I_p and F for selected integral energies of $E > 10$, > 30, > 60, and > 100 MeV.

Papaioannou *et al.* (2016) conveniently list the I_p in pfu and F in $\mathrm{cm}^{-2}\,\mathrm{sr}^{-1}$ for each of the four energy ranges with measurable increases for those 314 events in their Table 3. The event-onset times were determined with an algorithm that measures standard deviations [σ] of counting rates in selected time intervals and requires some multiple of σ above background for a specified number of intervals (Papaioannou *et al.*, 2014), but the event end times appear to be manually selected, and there is no discussion of whether or how detector counting-rate backgrounds were dealt with. Their accompanying Table 2 gives the associated flare characteristics for each SEP event where an association could be made.

Figure 7 shows log F *versus* log I_p for the four energy ranges of all their Table 3 SEP events. As with the other SEP data sets, we show the longitudinal groupings for the four energy ranges in Figures 8 and 9 along with the least-squares best fits and CCs. Some of the events of Figure 7 do not appear in Figures 8 and 9 because of a lack of solar-flare longitude associations.

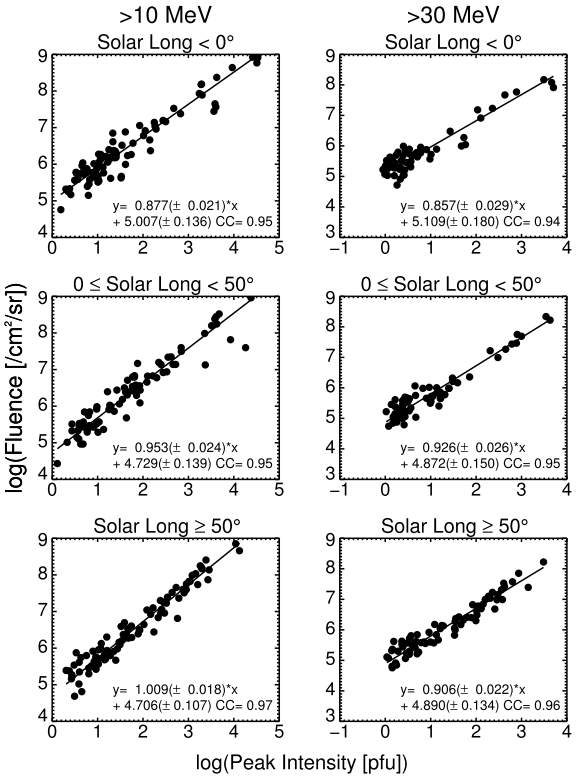

Figure 8 Log F *versus* log I_p in three longitude ranges of solar sources for the $E > 10$ MeV and $E > 30$ MeV ranges of the SEP events of Figure 7.

4. Results

4.1. Range and Slopes of Linear Fits

We first ask how F scales with I_p for the various groups of SEP events. In all of the log F *versus* log I_p plots of the three event studies, we performed linear least-squares fits over nearly (Figures 5 and 6) or more than (Figures 2 and 3 and 7 – 9) four orders of magnitude and found good results, as indicated by the high (≥ 0.90) CC-values given in the Figures and Table 1. Thus, over a very wide range of event I_p, these linear fits allow one to make estimates of the event fluences from observed I_p to within a factor of ≈ 1.6 ($\sigma = 0.2$ in the log). This close correlation is perhaps unexpectedly better than the larger implied range of I_p for fixed values of F shown in Figure 1 for the 14 selected $E > 50$ MeV events of KL.

We can examine the longitudinal variation of the log F *versus* log I_p relationship best through the unity-slope amplitudes of Table 1. The bottom panel of Figure 10 shows a clear trend for increased F amplitude values from western to eastern hemisphere SEP events. This might be expected from the higher eastern-hemisphere values of the event scaling parameter [β] plotted in Figure 7 of KL, which also shows little variation across the western hemisphere. Their figure is limited to only 14 events, but it is consistent with the relatively higher F-values for eastern events in Figure 10. This result is also in accord with the longitudinal variation of the median TD parameter of Table 3 of Kahler (2013), which decreases from 26 hours in the E130° – E06° range to 12 hours in the W33° – W90° ranges.

Are the best-fit slopes consistent with unity for all SEP energy ranges? The top panel of Figure 10 shows the derived slopes as functions of the mean longitudes for SEP event groups

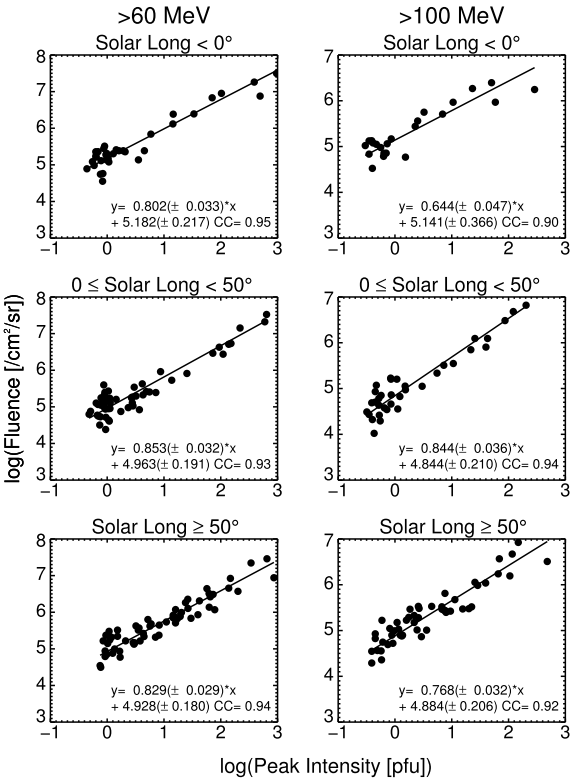

Figure 9 Log F *versus* log I_p in three longitude ranges of solar sources for the $E > 60$ MeV and $E > 100$ MeV ranges of the SEP events of Figure 7.

of Table 1. All of the slope fits to the Lario *et al.* and KWL events are within 2σ of unity, with no clear suggestion of variation with either energy or longitude. This is not the case for the Papaioannou *et al.* events, which consistently show slopes < 1. There is further a trend of decreasing slope with increasing energy, from 0.94 ± 0.01 for the $E > 10$ MeV events to 0.77 ± 0.02 for the $E > 100$ MeV events. This result is generally true in all longitude ranges, as seen in the top panel of Figure 10, and it suggests that with increasing event I_p at the highest energies, the associated event timescales may be decreasing.

The obvious discrepancy in the plots of the three data sets is between the slopes consistent with unity seen in the data of Lario *et al.* (Figures 2 and 3) and KWL (Figures 5 and 6) and the slopes of < 1 of Papaioanna *et al.* (Figures 7–9). The period 1986 to 2013 is common to the KWL and Papaioannou *et al.* studies, allowing direct comparisons of I_p and F for events common to the two data sets. We select as the closest energy match to the KWL $E > 50$ MeV events the $E > 60$ MeV events of Papaioannou *et al.* (2016). Our comparison of the two event lists yields 108 common SEP events. The top panel of Figure 11 compares event I_p of the two energy ranges. The slope is consistent with unity, as expected, but the log offset of 0.421 is a factor 2.64 in the ratio of the two integral I_p-values. If we assume all events to be fitted with a differential power law of the form

$$dN/dE = A \times E^{-\gamma}, \tag{2}$$

then $I_p(E > 50\,\text{MeV})/I_p(E > 60\,\text{MeV}) = 2.64$ implies that $\gamma = 6.33$, which is much higher than typical SEP event spectral indices of $\approx$ 1to 5 (Mewaldt *et al.*, 2012; Lee, Mewaldt, and

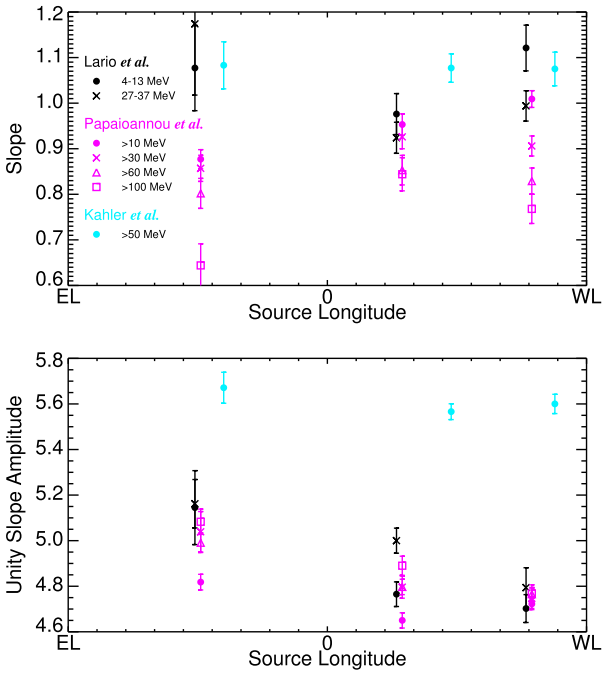

Figure 10 *Top*: Least-squares slopes of the fits as functions of the solar-source mid-longitude ranges of the events. The data points are *color-coded* by study and indicated by different *symbols* by energy ranges. *Bottom*: Study-specific SEP fluence amplitudes *versus* source longitudes when fitted with assumed slopes of unity. All data points are listed in Table 1.

Giacalone, 2012; Park *et al.*, 2015; Desai *et al.*, 2016; Gopalswamy *et al.*, 2016; Reames, 2017).

Perhaps more meaningful is the comparison of common event values of F shown in the bottom of Figure 11. Again we might expect a slope close to unity, but now it clearly exceeds that value, suggesting possibly that for events of larger I_p, the timescales at $E > 50$ MeV are increasing faster than those of $E > 60$ MeV. It seems more likely that the $E > 50$ MeV F are systematically overestimated or that the $E > 60$ MeV F are underestimated with increasing F (or both). We note that at the high-F range, where $\log(E > 60\ \text{MeV}) = 6.5$, then $\log(E > 50\ \text{MeV}) = 8.0$, a ratio of 32, which seems much too high, even with the energy-threshold difference. From these comparisons, it appears that the Papaioannou *et al.* method of recalculating or using the energy spectral data to obtain F may have given rise to systematic differences from the more straightforward approach of Lario *et al.* and KWL simply to integrate a given time series of standard computed integral energies, although in both cases the result remains a tight correlation between F and I_p.

We can perform a limited check of this apparent discrepancy by using the 16 $E >$ 30 MeV F-values presented in Table 2 of Mewaldt *et al.* (2012) for ground-level events (GLEs) of Solar Cycle 23. The F-values of these 16 events are included at the same energy threshold in the Papaioannou *et al.* list, so we expect matching values in this case. The plot of $\log F$ for these events is shown in Figure 12, again with the Papaioannou *et al.* values along the x-axis. As in the bottom of Figure 11, we obtain a slope > 1, and at plot mid-range ($x = 7$), we obtain an F-ratio of ≈ 30. We found the F/I_p slopes to decrease with increasing E in the Papaioannou *et al.* plots (Figures 7–9), so if the $E > 50$ MeV F of KWL are plotted consistently with the $E > 30$ MeV F of Mewaldt *et al.* (2012), the comparisons with the Papaioannou *et al.* F should yield increasing slopes with increasing E, as is the case with the two plots.

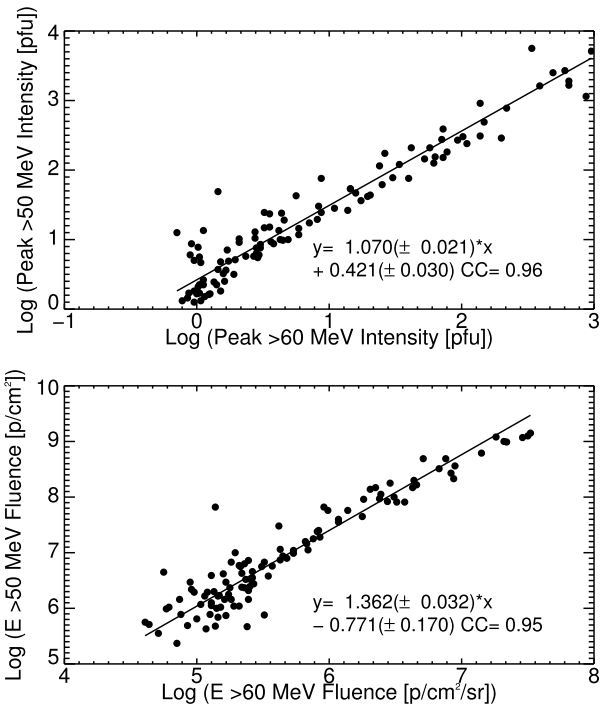

Figure 11 *Top*: Log–log plot of the $E > 50$ MeV I_p from KWL *versus* $E > 60$ MeV I_p from Papaioannou *et al.* (2016) for the 108 SEP events common to the two studies. The *diagonal line* is the least-squares best fit. *Bottom*: Log–log plot of F for the same set of SEP events. The least-squares fits and CCs are given in each panel.

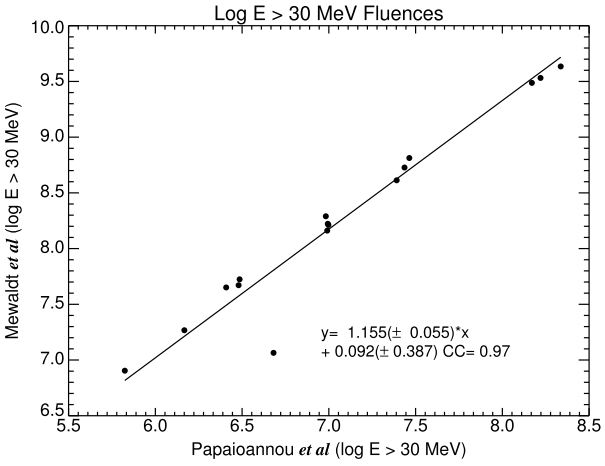

Figure 12 Log–log plot of the $E > 30$ MeV F from the GLEs of Mewaldt *et al.* (2012) *versus* $E > 30$ MeV F from Papaioannou *et al.* (2016) for the 16 SEP events common to the two studies. The *diagonal line* is the least-squares best fit, and the least-squares fits and CCs are given.

5. Discussion

The main result of this work is that there is a close linear relationship between the logs of F and I_p for large $E > 10$ MeV proton events. This result holds over about four orders of magnitude, but it has not been tested at the low ($E < 10$ MeV nuc^{-1}) energies and small I_p and F that characterize impulsive SEP events (Reames, 2017). Nor has this relationship been tested for energetic electrons, He, or heavy-Z ions of any SEP events, or at the highest $E > 500$ MeV range of GLEs. As discussed in the Introduction, F is an important SEP-event

parameter for understanding the shock energetics and perhaps the seed-particle population of SEP events, as well as for modeling SEP events. The problem of accounting for both the adiabatic energy losses and multiple traversals of particles in calculating F has been addressed by Chollet, Giacalone, and Mewaldt (2010), who found that the two effects are generally equal and offsetting for a broad range of energies and over many ion species. Their work does not suggest the slopes of $<$ unity or the slope-energy dependence that we found in the Papaioannou *et al.* plots.

It is therefore important to understand the source of the difference between the conflicting slopes of ≈ 1 or < 1 of the $F-I_{\rm p}$ correlations that we found here. The F- and $I_{\rm p}$-values of Papaioannou *et al.* were calculated using values of the energy ranges of the EPS P2 to P7 detectors on the GOES spacecraft revised downward after extensive comparisons with IMP-8 detectors (Sandberg *et al.*, 2014). Recent intercomparisons of the EPS detectors on the different GOES spacecraft (Rodriguez, Krosschell, and Green, 2014) and comparisons with the *Solar Terrestrial Relations Observatory* (STEREO) *Low Energy Telescope* (LET) and *High Energy Telescope* (HET) detectors (Rodriguez *et al.*, 2017) have further refined the EPS detector-energy ranges, but these systematically revised values should not affect the basic results of the log–log F *versus* $I_{\rm p}$ plots discussed here.

In the context of shock acceleration, the simple interpretation of the Papaioannou *et al.* result is that events with higher $I_{\rm p}$ are produced over decreasing timescales, *i.e.* more impulsively, while the unity-slope result suggests a simple scaling up of SEP injections over comparable timescales. In either case, it is important that any use of the linear correlations shown here to deduce F from $I_{\rm p}$ is subject to a significant uncertainty that is due to the two basic correlation results.

We have not related the basic $F-I_{\rm p}$ correlation to the two-parameter fits of SEP event $I(t)$ profiles discussed in Section 2. In the 14 SEP events examined by KL, there appeared to be large variations of the modified Weibull-function fit parameters α and β that would not suggest the good $F-I_{\rm p}$ correlations found here. The fitting of more SEP events may reveal unexpected limitations or correlations between the fitting parameters consistent with the $F-I_{\rm p}$ correlation.

6. Conclusion

Solar energetic particle event fluences $[F]$ are important both for determining the amount of radiation doses on components of space systems and for understanding the physics of shock acceleration and transport. It is usually assumed that there is no close dependence of F on $I_{\rm p}$, so integrations of $I(t)$ over each event duration must be carried out. In our examination of three studies in which these integrations were carried out, we find a very robust statistical linear correlation between logs of F and $I_{\rm p}$ over an energy range from > 10 MeV to > 100 MeV and over four decades of F and $I_{\rm p}$. However, the Papaioannou *et al.* (2016) data revealed slopes of < 1 and decreasing with increasing energy, while the other two data sets were consistent with energy-independent slopes of unity. In both cases, the $F/I_{\rm p}$ ratios increased slightly for SEP events from western- to eastern-longitude sources.

Acknowledgements S. Kahler was funded by AFOSR Task 2301RDZ4. A. Ling was supported by AFRL contract FA9453-12-C-0231.

Disclosure of Potential Conflicts of Interest The authors declare that they have no conflicts of interest.

References

Aschwanden, M.J., Caspi, A., Cohen, C.M.S., Holman, G., Jing, J., Kretzschmar, M., *et al.*: 2017, *Astrophys. J.* **836**, 17. DOI.

Bain, H.M., Mays, M.L., Luhmann, J.G., Li, Y., Jian, L.K., Odstrcil, D.: 2016, *Astrophys. J.* **825**, 1. DOI.

Balch, C.: 2008, *Space Weather* **6**, S01001. DOI.

Belov, A.: 2009, *Adv. Space Res.* **43**, 467. DOI.

Cane, H.V., Richardson, I.G., von Rosenvinge, T.T.: 2010, *J. Geophys. Res.* **115**, A08101. DOI.

Chollet, E.E., Giacalone, J., Mewaldt, R.A.: 2010, *J. Geophys. Res.* **115**, A06101. DOI.

Cohen, C.M.S., Mason, G.M., Mewaldt, R.A.: 2017, *Astrophys. J.* **843**, 132. DOI.

Desai, M.I., Mason, G.M., Dayeh, M.A., Ebert, R.W., McComas, D.J., Li, G., Cohen, C.M.S., Mewaldt, R.A., Schwadron, N.A., Smith, C.W.: 2016, *Astrophys. J.* **828**, 106. DOI.

Emslie, A.G., Dennis, B.R., Shih, A.Y., Chamberlin, P.C., Mewaldt, R.A., Moore, C.S., Share, G.H., Vourlidas, A., Welsch, B.T.: 2012, *Astrophys. J.* **759**, 71. DOI.

Falconer, D., Barghouty, A.F., Khazanov, I., Moore, R.: 2011, *Space Weather* **9**, S04003. DOI.

Gopalswamy, N., Xie, H., Akiyama, S., Mäkelä, P.A., Yashiro, S.: 2014, *Earth Planets Space* **66**, 104. DOI.

Gopalswamy, N., Mäkelä, P., Akiyama, S., Yashiro, S., Xie, H., Thakur, N., Kahler, S.W.: 2015, *Astrophys. J.* **806**, 8. DOI.

Gopalswamy, N., Yashiro, S., Thakur, N., Mäkelä, P., Xie, H., Akiyama, S.: 2016, *Astrophys. J.* **833**, 216. DOI.

Ji, E.-Y., Moon, Y.-J., Park, J.: 2014, *J. Geophys. Res.* **119**, 9389. DOI.

Kahler, S.W.: 2013, *Astrophys. J.* **769**, 110. DOI.

Kahler, S.W., Ling, A.G.: 2017, *Solar Phys.* **292**, 59. DOI.

Kahler, S.W., Ling, A., White, S.M.: 2015, *Space Weather* **13**, 116. DOI.

Kahler, S.W., Vourlidas, A.: 2013, *Astrophys. J.* **769**, 143. DOI.

Kahler, S.W., Vourlidas, A.: 2014, *Astrophys. J.* **791**, 4. DOI.

Kahler, S.W., White, S.M., Ling, A.G.: 2017, *J. Space Weather Space Clim.* **7**, A27. DOI.

Lario, D., Karelitz, A.: 2014, *J. Geophys. Res.* **119**, 4185. DOI.

Lario, D., Kallenrode, M.-B., Decker, R.B., Roelof, E.C., Krimigis, S.M., Aran, A., Sanahuja, B.: 2006, *Astrophys. J.* **653**, 1531. DOI.

Lario, D., Aran, A., Gómez-Herrero, R., Dresing, N., Heber, B., Ho, G.C., Decker, R.B., Roelof, E.C.: 2013, *Astrophys. J.* **767**, 41. DOI.

Laurenza, M., Cliver, E.W., Hewitt, J., Storini, M., Ling, A.G., Balch, C.C., Kaiser, M.L.: 2009, *Space Weather* **7**, S04008. DOI.

Lee, M.A., Mewaldt, R.A., Giacalone, J.: 2012, *Space Sci. Rev.* **173**, 247. DOI.

Luhmann, J.G., Ledvina, S.A., Odstrcil, D., Owens, M.J., Zhao, X.-P., Liu, Y., Riley, P.: 2010, *Adv. Space Res.* **46**, 1. DOI.

Luhmann, J.G., Mays, M.L., Odstrcil, D., Li, Y., Bain, H., Lee, C.O., Galvin, A.B., Mewaldt, R.A., Cohen, C.M.S., Leske, R.A., Larson, D., Futaana, Y.: 2017, *Space Weather* **15**, 934. DOI.

Marsh, M.S., Dalla, S., Dierckxsens, M., Laitinen, T., Crosby, N.B.: 2015, *Space Weather* **13**, 386. DOI.

Mason, G.M., Li, G., Cohen, C.M.S., Desai, M.I., Haggerty, D.K., Leske, R.A., Mewaldt, R.A., Zank, G.P.: 2012, *Astrophys. J.* **761**, 104. DOI.

Mewaldt, R.A., Cohen, C.M.S., Giacalone, J., Mason, G.M., Chollet, E.E., Desai, M.I., Haggerty, D.K., Looper, M.D., Selesnick, R.S., Vourlidas, A.: 2008, *AIP* **CP-1039**, 111. DOI.

Mewaldt, R.A., Looper, M.D., Cohen, C.M.S., Haggerty, D.K., Labrador, A.W., Leske, R.A., Mason, G.M., Mazur, J.E., von Rosenvinge, T.T.: 2012, *Space Sci. Rev.* **171**, 97. DOI.

Miteva, R., Klein, K.-L., Malandraki, O., Dorrian, G.: 2013, *Solar Phys.* **282**, 579. DOI.

Papaioannou, A., Souvatzoglou, G., Paschalis, P., Gerontidou, M., Mavromichalaki, H.: 2014, *Solar Phys.* **289**, 423. DOI.

Papaioannou, A., Sandberg, I., Anastasiadis, A., Kouloumvakos, A., Georgoulis, M.K., Tziotziou, K., Tsiropoula, G., Jiggens, P., Hilgers, A.: 2016, *J. Space Weather Space Clim.* **6**, A42. DOI.

Park, J., Moon, Y.-J.: 2014, *J. Geophys. Res.* **119**, 9456. DOI.

Park, J., Innes, D.E., Bucik, R., Moon, Y.-J., Kahler, S.W.: 2015, *Astrophys. J.* **808**, 3. DOI.

Pomoell, J., Aran, A., Jacobs, C., Rodríguez-Gasén, R., Poedts, S., Sanahuja, B.: 2015, *J. Space Weather Space Clim.* **5**, A12. DOI.

Posner, A.: 2007, *Space Weather* **5**, S05001. DOI.

Reames, D.V.: 2014, *Solar Phys.* **289**, 977. DOI.

Reames, D.V.: 2015, *Space Sci. Rev.* **194**, 303. DOI.

Reames, D.V.: 2017, *Solar Energetic Particles: A Modern Primer on Understanding Sources, Acceleration and Propagation*, *Lect. Notes Phys.* **932**, Springer, Berlin. DOI.

Reames, D.V., Cliver, E.W., Kahler, S.W.: 2014, *Solar Phys.* **289**, 3817. DOI.

Richardson, I.G., von Rosenvinge, T.T., Cane, H.V., Christian, E.R., Cohen, C.M.S., Labrador, A.W., Leske, R.A., Mewaldt, R.A., Wiedenbeck, M.E., Stone, E.C.: 2014, *Solar Phys.* **289**, 3059. DOI.
Rodriguez, J.V., Krosschell, J.C., Green, J.C.: 2014, *Space Weather* **12**, 92. DOI.
Rodriguez, J.V., Sandberg, I., Mewaldt, R.A., Daglis, I.A., Jiggens, P.: 2017, *Space Weather* **15**, 290. DOI.
Sandberg, I., Jiggens, P., Heynderickx, D., Daglis, I.: 2014, *Geophys. Res. Lett.* **41**(13), 4435. DOI.
Schmelz, J.T., Reames, D.V., von Steiger, R., Basu, S.: 2012, *Astrophys. J.* **755**, 33. DOI.
Schwadron, N.A., Gorby, M., Török, T., Downs, C., Linker, J., Lionello, R., *et al.*: 2014, *Space Weather* **12**, 323. DOI.
Takahashi, T., Mizuno, Y., Shibata, K.: 2016, *Astrophys. J. Lett.* **833**, L8. DOI.
Verkhoglyadova, O.P., Li, G., Zank, G.P., Hu, Q., Cohen, C.M.S., Mewaldt, R.A., Mason, G.M., Haggerty, D.K., von Rosenvinge, T.T., Looper, M.D.: 2010, *J. Geophys. Res.* **115**, A12103. DOI.
Wilks, D.S.: 2006, *Statistical Methods in the Atmospheric Sciences*, 2nd edn. Elsevier, Boston.
Zelina, P., Dalla, S., Cohen, C.M.S., Mewaldt, R.A.: 2017, *Astrophys. J.* **835**, 71. DOI.